International Journal of Research
Available at https://edupediapublications.org/journals
e-ISSN: 2348-6848
p-ISSN: 2348-795X
Volume 05 Issue 15
May 2018

Improve the Power Quality in Electrical Railway Power System Using Fuzzy Logic Controller

Gadapa Naresh & P.Nageswara Rao

[1]M.Tech, (Student) Vidya Jyothi Institute of Technology (Autonomous), Hyderabad, Telangana, India
[2]Associate Professor Dept. of EEE, Vidya Jyothi Institute Of Technology (Autonomous), Hyderabad India

ABSTRACT- *This paper is to create Power Quality in Electric Railway systems with the assistance of Fuzzy Logic controller. Concentrating on the cargo prepare prevailing electrical railroad power system (ERPS) blended with air conditioning dc and air conditioning dc-air conditioning trains (its power factorϵ[0.70,0.84]), this paper proposes a power factor situated railroad power flow controller (RPFC) for the power quality improvement of ERPS. In this paper the thorough relationship of the primary power factor, converter limit, and the two phase load currents are introduced. By this technique we can likewise control the power flow trade between the grid and the load, with the goal that instantaneous active and reactive power is maintain constant. Moreover, as the main commitment of this paper, the ideal remunerating procedure suited the irregular varied two phase loads is broke down and planned based on a genuine footing substation, for the reasons for fulfilling the power quality standard, improving RPFC's control adaptability, and diminishing converter's ability. Here we are utilizing the fuzzy controller contrasted with different controllers i.e. The fuzzy controller is the most reasonable for the human basic leadership component, giving the operation of an electronic system with choices of specialists. What's more, utilizing the fuzzy controller for a nonlinear system takes into account a decrease of indeterminate impacts in the system control and enhances the effectiveness. By utilizing simulation results we can examine the improvement of the power quality in electric railroad systems utilizing fuzzy logic controller.*

Index Terms—Power factor; negative sequence; power quality; power flow controller; electrical railway power system; converter, Fuzzy logic controller.

INTRODUCTION

Power quality has become an increasing concern in railway systems. Poor power quality affects the performance, reliability of the railway system as well as having an effect on equipment attached to the local distribution network. The analysis of power quality on a rail system is essential, to enable the analysis of train performance and to assess the effects of a rail system on the adjacent distribution network. Railway systems are electrically complex. The loads, trains, are constantly moving and their electrical behaviour is constantly changing. Modelling is an ideal tool to analyse the power quality of such a complex system. An ideal model would be accurate yet computationally efficient.

As the popular PQ improvement rig, static Var compensator (SVC) static synchronous compensator (STATCOM) active filter transformer integrated power conditioner, railway power flow controller (RPFC) and the well-designed train-mounted front end rectifier are commonly used in ERPS. Considering the comprehensive performance, RPFC is concerned greatly by related departments due to its compatibility – it can, unlike the above rigs, integrate in the secondary side of almost all kinds of traction transformer. By rebalancing the two phase active power, and compensating the reactive power or harmonics in each phase independently, RPFC can deal with almost all the main PQ problems of ERPS. Additionally, the feeder voltage's stability and the capacity utilization ratio of the main transformer can also be enhanced significantly which are attractive for improving ERPS's transport capacity and cost-efficiency.

Power Quality has to be considered from two perspectives, the railway system and the local distribution network to which it is attached. Poor power quality on the railway system affects performance limits capacity and may introduce a need for additional maintenance. Distribution network operators stipulate power quality standards. Railway systems are required to meet these standards. Power quality is divided into categories [1]. Railway systems typically suffer from poor voltage regulation and harmonic distortion. Voltage regulation affects the performance of traction units and imposes a capacity limit on the system. Harmonic distortion can cause damage to traction units, particularly motors [2]. Rail systems can cause harmonic distortion and voltage unbalance on the local distribution network. The harmonic distortion is caused by the non-linear currents drawn by the railway system and in DC systems by rectifying substations. Voltage unbalance is present in AC systems, where the rail system draws large currents from a single phase of the supply.

International Journal of Research
Available at https://edupediapublications.org/journals
e-ISSN: 2348-6848
p-ISSN: 2348-795X
Volume 05 Issue 15
May 2018

For amplifying blocking NSC, another repaying system was proposed in [30]. It centers around the theme of limiting NSC for a given RPFC's ability, in other words, it has no assistance on the limit assurance in the planning phase of RPFC. Furthermore, considering the short out limit Sd of a footing substation is constantly composed inside 500-1500MVA, we found in the pragmatic designing project that, after a little measure of pay, the standard of Vunb% can be effectively accomplished than the prerequisite of PF, particularly for V/v transformer (note: Vunb%=1.732VNI-/Sd; VN: primary typical line voltage, I-: NSC). In other words, the reactive power ought to be affirmed to be the main repaying focus of RPFC in the air conditioner dc train prevailing ERPS with blended trains, the regulation of NSC, at that point, debases into the subordinate one, however can't be disregarded.

To additionally enhance RPFC's ability usage capacity and control adaptability in both outlining and working stages in cargo prepare overwhelming ERPS, in this paper, we will center around the arrangement of the accompanying perspectives:

1) Establishing the connection between the primary PF with RPFC's remunerating limit; the converter's ability can be adaptably composed by modifying the primary PF.

2) In the commence of limiting RPFC's ability for a given PF, considering an ideal control system to diminishing NSC and NSV in a satisfactory level.

3) The proposed control procedure ought not exclusively be connected in the basic single phase ERPS, yet in addition in the vital regular utilized two phase system (see Fig.1).

This paper is sorted out as takes after, the mathematical model of the RPFC coordinated two phase ERPS is displayed in Section II. In the introduce of relief NSC, as the main commitment of this paper, Section III gives the PF situated ideal pay system for RPFC. Simulation are given in Section IV and V. Segment VI is the conclusion.

II. GENERAL MATHEMATICAL MODEL OF RPFC INTEGRATED IN TWO PHASE ERPS

Initially, we characterize the casing ABC by the V/v transformer's primary three phase voltage VA, VB, and VC, i.e., Frame-ABC:

$$\mathbf{V}_A = V_p\angle 0^\circ, \mathbf{V}_B = V_p\angle -120^\circ, \mathbf{V}_C = V_p\angle -240^\circ \qquad (1)$$

Where, V p is the root mean square (RMS) estimation of VA, VB, and VC. Reference to Fig. 1, the phasor diagram of the V/v transformer based ERPS can be acquired, as appeared in Fig. 2.

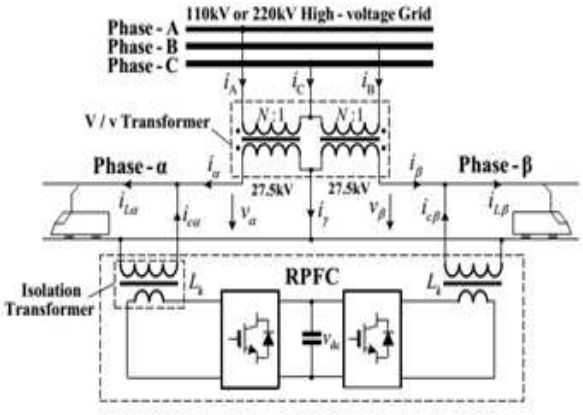

Fig. 1. The typical RPFC integrated two phase ERPS (V/v transformer is adopted as the main transformer).;

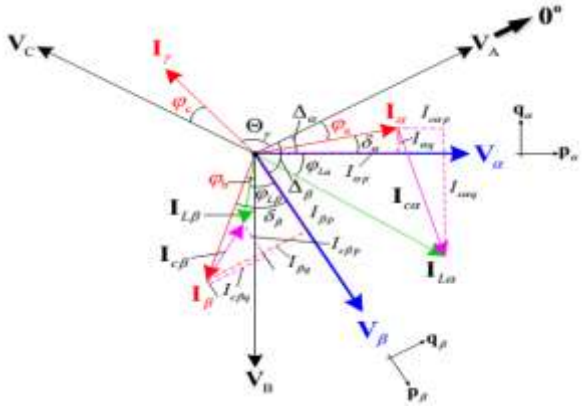

Fig. 2. The phasor diagram of the V/v transformer based ERPC with RPFC.

From Fig. 2, we define the PF in phase-A, B, and C, i.e., PFA~PFC as:

$$PF_A = \cos\varphi_a, PF_B = \cos\varphi_b, PF_C = \cos\varphi_c \qquad (2)$$

Where , φk>0 means that the present slacks the voltage, generally, the present leads the voltage (k=a, b, c). It can be seen from Figs. 1 and 2 that, the output currents Iα and I β of the V/v transformer in outline pαqα and outline pβqβ (see Fig.2) can be

International Journal of Research
Available at https://edupediapublications.org/journals
e-ISSN: 2348-6848
p-ISSN: 2348-795X
Volume 05 Issue 15
May 2018

communicated as

$$\begin{cases} \mathbf{I}_{\alpha} = \mathbf{I}_{L\alpha} - \mathbf{I}_{c\alpha} = \underbrace{(I_{L\alpha p} - I_{c\alpha p})}_{I_{\alpha p}} + j\underbrace{(I_{L\alpha q} - I_{c\alpha q})}_{I_{\alpha q}} \\ \mathbf{I}_{\beta} = \mathbf{I}_{L\beta} - \mathbf{I}_{c\beta} = \underbrace{(I_{L\beta p} - I_{c\beta p})}_{I_{\beta p}} + j\underbrace{(I_{L\beta q} - I_{c\beta q})}_{I_{\beta q}} \end{cases}, \quad (3)$$

Where, subscript "p" and "q" speaks to the active and reactive component of the relating variable in outline pαqα or outline pβqβ, separately. Furthermore, Fig. 2 additionally demonstrates that the relationship of the p, q components of Iα and Iβ in outline pαqα and pβqβ fulfill:

$$\begin{cases} I_{\alpha q} = I_{\alpha p}\tan\delta_{\alpha} = (I_{L\alpha p} - I_{c\alpha p})\tan\delta_{\alpha} \\ I_{\beta q} = I_{\beta p}\tan\delta_{\beta} = (I_{L\beta p} - I_{c\beta p})\tan\delta_{\beta} \end{cases}, \quad (4)$$

$$\text{where} \begin{cases} \delta_{\alpha} = \Delta_{\alpha} - \varphi_{\mathrm{a}} \\ \delta_{\beta} = \Delta_{\beta} - \varphi_{\mathrm{b}} - 120^{\circ} \end{cases}.$$

Note: for V/v transformer, Δα=30° , Δβ=90°.

Disregarding the converter's losses, and accepting Vα=Vβ, the active power adjust of the consecutive converter can lead the consequence of:

$$I_{c\alpha p} = -I_{c\beta p}. \quad (5)$$

Then again, Fig. 2 shows that Iγ's phase point Θγ in outline ABC fulfil

$$\Theta_{\gamma} = 120^{\circ} - \varphi_{\mathrm{c}} \text{ or } \tan\Theta_{\gamma} = \tan(120^{\circ} - \varphi_{\mathrm{c}}). \quad (6)$$

Based on the Kirchhoff's law, Iα, Iβ, and Iγ in outline ABC I α ABC , $I\beta_{ABC}$, and $I\gamma_{ABC}$ fulfill

$$-\mathbf{I}_{\gamma} = -\mathbf{I}_{\gamma}^{\mathrm{ABC}} = \mathbf{I}_{\alpha}^{\mathrm{ABC}} + \mathbf{I}_{\beta}^{\mathrm{ABC}}, \quad (7)$$

Where

$$\begin{cases} \mathbf{I}_{\alpha}^{\mathrm{ABC}} = \mathbf{I}_{\alpha}\angle -\Delta_{\alpha} \\ \mathbf{I}_{\beta}^{\mathrm{ABC}} = \mathbf{I}_{\beta}\angle -\Delta_{\beta} \end{cases}. \quad (8)$$

Substituting (3), (4), and (8) into (7), the genuine and nonexistent piece of - Iγ, Term-I and Term-II, can be computed as

$$\begin{cases} \text{Term-I} = I_{\alpha p}\cos\Delta_{\alpha} + I_{\alpha q}\sin\Delta_{\alpha} + I_{\beta p}\cos\Delta_{\beta} + I_{\beta q}\sin\Delta_{\beta} \\ \text{Term-II} = -I_{\alpha p}\sin\Delta_{\alpha} + I_{\alpha q}\cos\Delta_{\alpha} - I_{\beta p}\sin\Delta_{\beta} + I_{\beta q}\cos\Delta_{\beta} \end{cases} \quad (9)$$

Substituting (9) into (6), and considering the expressions of Iα p, Iαq, Iβp, and Iβq in (3)-(5), the relationship of $I_{c\alpha p}$ with the two phase load active currents $I_{L\alpha p}$ and $I_{L\beta p}$ can be calculated as

$$I_{c\alpha p} = \underbrace{\frac{x_1}{x_1 + x_2}}_{\mu_{\alpha}} I_{L\alpha p} - \underbrace{\frac{x_2}{x_1 + x_2}}_{\mu_{\beta}} I_{L\beta p}, \quad (10)$$

Where

$$\begin{cases} x_1 = \sin\theta_{\alpha} - \cos\theta_{\alpha}\tan\delta_{\alpha} \\ x_2 = \cos\theta_{\beta}\tan\delta_{\beta} - \sin\theta_{\beta} \end{cases}, \begin{cases} \theta_{\alpha} = \Delta_{\alpha} - \varphi_{\mathrm{c}} + 120^{\circ} \\ \theta_{\beta} = \Delta_{\beta} - \varphi_{\mathrm{c}} + 120^{\circ} \end{cases}.$$

Re-substituting (10) into (3)- (5), the remunerating currents of RPFC can be acquired as

$$\begin{cases} I_{c\alpha p} = \mu_{\alpha} I_{L\alpha p} - \mu_{\beta} I_{L\beta p} \\ I_{c\beta p} = -\mu_{\alpha} I_{L\alpha p} + \mu_{\beta} I_{L\beta p} \\ I_{c\alpha q} = -[\tan\varphi_{L\alpha} + (1-\mu_{\alpha})\tan\delta_{\alpha}]I_{L\alpha p} - \mu_{\beta}\tan\delta_{\alpha} I_{L\beta p} \\ I_{c\beta q} = \mu_{\alpha}\tan\delta_{\beta} I_{L\alpha p} - [\tan\varphi_{L\beta} + (1+\mu_{\beta})\tan\delta_{\beta}]I_{L\beta p} \end{cases}. \quad (11)$$

Increasing the feeder voltage Vα or Vβ in the two sides of (11), RPFC's remunerating power in phase α and β, i.e., Pcα, Qcα and Pcβ, Qcβ, can be ascertained as

$$\begin{cases} P_{c\alpha} = \mu_{\alpha} P_{L\alpha} - \mu_{\beta} P_{L\beta} \\ P_{c\beta} = -\mu_{\alpha} P_{L\alpha} + \mu_{\beta} P_{L\beta} \\ Q_{c\alpha} = -[\tan\varphi_{L\alpha} + (1-\mu_{\alpha})\tan\delta_{\alpha}]P_{L\alpha} - \mu_{\beta}\tan\delta_{\alpha} P_{L\beta} \\ Q_{c\beta} = \mu_{\alpha}\tan\delta_{\beta} P_{L\alpha} - [\tan\varphi_{L\beta} + (1+\mu_{\beta})\tan\delta_{\beta}]P_{L\beta} \end{cases} \quad (12)$$

Where, $P_{L\alpha}$ and PLβ are the load's active power in phase α and β. It can be seen from (12), in light of the fact that Δα, Δβ can be pre-acquired for a specific sort of a transformer (e.g., the V/v transformer and other sort of the adjust transformers [35], [36]), μα and μβ are just dictated by PFA~PFC or φa~φc [see (10) and (2)]. Henceforth, the active and reactive power of the RPFC can be adaptably balanced by controlling the primary three phase power factors, if the PFs of the two phase loads are pre-ascertained [see $\varphi_{L\alpha}$ and $\varphi_{L\beta}$ in (12)], which will be talked about later on.

III. COMPENSATING STRATEGY DESIGN

A.The Possible Compensating Scheme:

International Journal of Research
Available at https://edupediapublications.org/journals
e-ISSN: 2348-6848
p-ISSN: 2348-795X
Volume 05 Issue 15
May 2018

For the consideration of planning accommodation and the necessity of PF≥0.9, we let

$$\begin{cases} |\varphi_a| = |\varphi_b| = |\varphi_c| \\ PF^* = \cos\varphi_k \in [0.9,1],\ k=a,\ b,\ c \end{cases}, \quad (13)$$

Where PF* is the primary reference power factor. It can be observed from Fig. 2 that Iα, Iβ, and Iγ (or IA, IB, and IC) may leads or slacks VA, VB, and VC, individually, which means eight (i.e., 8=23) conceivable combination models with positive or negative esteem are existed in φa, φb, and φc. In addition, Fig. 2 additionally demonstrates the reactive power of converter-α is bigger than the one created by converter-β (i.e., Icαq>Icβq), to lessen the VA-limit of converter-α, Iα must be confined slacking than VA (i.e., φa>0), so the over eight conceivable combination models of φa~φc will decline into four profitable hopefuls, which are recorded in Table I (i.e., Model-2 to - 5).

Table I
Compensating Scheme OfRpfc

Compensating model	φ_a	φ_b	φ_c
Model-1 (i.e., FCM)	0	0	0
Model-2	>0	<0	>0
Model-3	>0	<0	<0
Model-4	>0	>0	>0
Model-5	>0	>0	<0

* φ_k>0 (or <0) means the inductive (or capacitive) PF (k=a, b, and c).

B. Compensating Capacity Analysis:
The VA-capacity SRPFC of the RPFC is:

$$S_{RPFC} = \underbrace{\sqrt{P_{c\alpha}^{\ 2} + Q_{c\alpha}^{\ 2}}}_{S_{converter-\alpha}} + \underbrace{\sqrt{P_{c\beta}^{\ 2} + Q_{c\beta}^{\ 2}}}_{S_{converter-\beta}} \quad (14)$$

Substituting (12) into (14), the RPFC's VA-limit in the five repaying model recorded in Table I are appeared in Fig. 3 [PLα and PLβ are the two phase loads' active power,

PF*=0.95, and the two phase loads' PF=0.8 (from a substation's data)]. It can be seen from Fig. 3(a) that, the VA-limit of RPFC has a place with five unique surfaces in Model-1~5 individually. The maximum SRPFC happens in the single phase loaded condition, in which Model-1, 2, and 4 compare to PLα≠0, PLαβ=0, while the contrary circumstance has a place with Model-3 and 5.

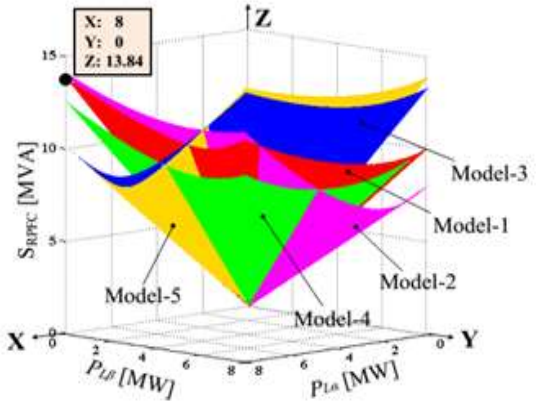

(a)

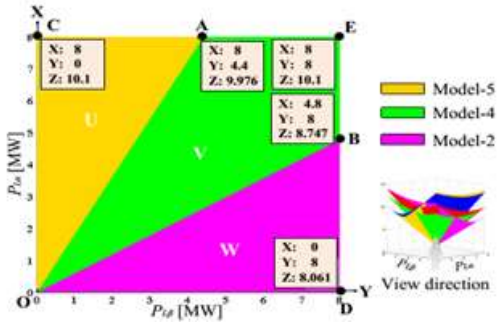

(b)

Fig. 3. The relationship of SRPFC with the two phase loads' active power in the five valuable compensating models. (a) The surfaces of SRPFC with the two phase loads' active power. (b) The xoy-projection of the surfaces in Fig. 3(a).

Also, a surface joined by the surfaces of Model-2, 4, and 5 has the base SRPFC. Contrasted and Model-1, i.e., FCM, the limit diminishing ratio of this grafted surface is around 30%, which can influence the converter to have higher system unwavering quality and proficiency. In this way, it can be chosen as the ideal repaying surface. In the event that PF*=0.95, from Fig. 3(b) the ideal remunerating methodology (OCS) can be preparatory communicated as

$$\mathbf{OCS}|_{PF^*=0.95}: \begin{cases} \text{Model-5},\ 0\text{MW} \le P_{L\beta} < 0.55P_{La} \\ \text{Model-4},\ 0.55P_{La} \le P_{L\beta} \le 1.67P_{La} \\ \text{Model-2},\ 1.67P_{La} < P_{L\beta} \le 8\text{MW} \end{cases}. \quad (15)$$

International Journal of Research
Available at https://edupediapublications.org/journals
e-ISSN: 2348-6848
p-ISSN: 2348-795X
Volume 05 Issue 15
May 2018

C.The NSC Mitigation Ability Analysis

But of remunerating reactive power, alleviation of the NSC is another motivation behind RPFC. In other words, a satisfactory repaying technique ought to limit SRPFC, as well as has the obligation to diminish NSC inside a satisfactory level.

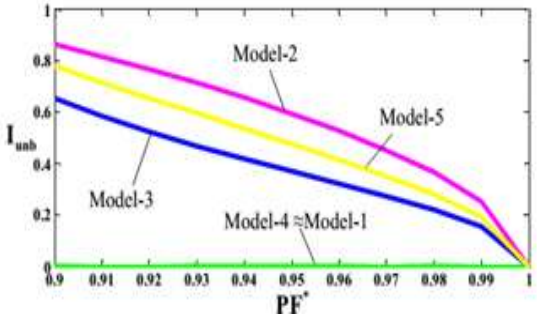

Fig. 4.The curves of I_{unb} v.s. PF of Model-1~5.

Brushing (7)- (8), the primary positive and negative sequence currents, I+ and I-, can be found by

$$\begin{bmatrix}\mathbf{I}_+\\ \mathbf{I}_-\end{bmatrix}=\frac{1}{3N}\begin{bmatrix}1 & \xi & \xi^2\\ 1 & \xi^2 & \xi\end{bmatrix}\begin{bmatrix}\mathbf{I}_\alpha^{ABC}\\ \mathbf{I}_\beta^{ABC}\\ \mathbf{I}_\gamma^{ABC}\end{bmatrix}$$
$$=\frac{\mu_\beta(I_{La_P}+I_{L\beta_P})(1+j\tan\delta_\alpha)}{\sqrt{3}N}\begin{bmatrix}\angle-(\Delta_\alpha-30^\circ)\\ \angle-(\Delta_\alpha+30^\circ)\end{bmatrix}+\frac{\mu_\alpha(I_{La_P}+I_{L\beta_P})(1+j\tan\delta_\beta)}{\sqrt{3}N}\begin{bmatrix}\angle-(\Delta_\beta-90^\circ)\\ \angle-(\Delta_\beta+90^\circ)\end{bmatrix} \quad (16)$$

Where, ξ=∠120° , N= VsN/VfN is the turn's ratio of the main transformer (VsN and VfN are the grid and feeder typical line voltage separately; as appeared in Fig. 1).

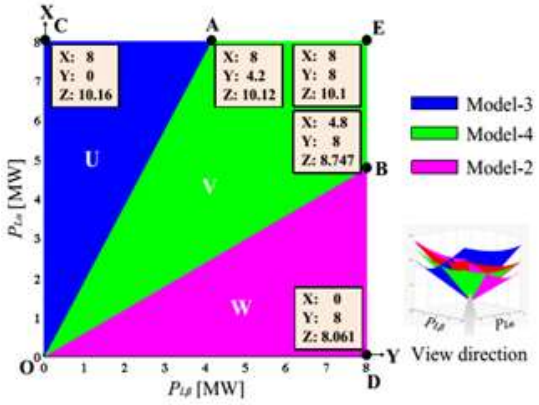

Fig. 5.The optimal compensating strategy of considering the NSC suppressing ability

From (16), the present unbalance ratio Iunb (Iunb=I-/I+) can be gotten as takes after.

$$I_{unb}=\sqrt{\frac{\mu_\alpha^2\cos^2\delta_\alpha+\mu_\beta^2\cos^2\delta_\beta+2\mu_\alpha\mu_\beta\cos\delta_\alpha\cos\delta_\beta\cos(\varphi_a-\varphi_b-180^\circ)}{\mu_\alpha^2\cos^2\delta_\alpha+\mu_\beta^2\cos^2\delta_\beta+2\mu_\alpha\mu_\beta\cos\delta_\alpha\cos\delta_\beta\cos(\varphi_a-\varphi_b-60^\circ)}} \quad (17)$$

From (13), (17), and Table I, the relationship of Iunb and PF* of Model-1~ 5 are appeared in Fig. 4. From Fig. 4 and Fig. 3 (a), we can observe that, however the limit surfaces of Model-3 and 5 are close [Fig. 3 (a)], the NSC stifling capacity of Model-3 is superior to that of Model-5 (Fig. 4). It demonstrates that, if Model-5 is substituted by Model-3, RPFC can show signs of improvement NSC stifling capacity with nearly has a similar VA-limit of Model-5. In other words, the remunerating procedure joined of Model-2, 4, and 3 has higher exhaustive execution than the one consolidated by Model-2, 4, and 5. So the certified OCS ought to be adjusted from Fig. 3(b) into Fig. 5, and its determination is given in (18).

$$\mathbf{OCS}\big|_{PF^*=0.95}:\begin{cases}\text{Model-3, } 0\text{MW}\le P_{L\beta}<0.415P_{L\alpha}\\ \text{Model-4, } 0.55P_{L\alpha}\le P_{L\beta}\le 1.67P_{L\alpha}\\ \text{Model-2, } 1.67P_{L\alpha}<P_{L\beta}\le 8\text{MW}\end{cases} \quad (18)$$

Fig. 6 gives the slants of line OA and OB, i.e., KOA and KOB in various PF* (note: OA and OB are the limits of the three remuneration demonstrate appeared in Fig. 5; the loads' PF are as yet affirmed to be 0.8, on the grounds that the power factor changes in a little rang around 0.8 in the deliberate substation). It can be observed from Fig. 6 that, KOA's change amplitude is 0.114, while, it fluctuates in generally expansive range for KOB. For execution of the proposed OCS, a satisfactory execution can likewise be acquired by settling KOA on 0.5, and modifying KOB by PF* concurring the blue bend appeared in Fig. 6. It can be pre-implanted in the advanced controller's memory space in useful

International Journal of Research
Available at https://edupediapublications.org/journals
e-ISSN: 2348-6848
p-ISSN: 2348-795X
Volume 05 Issue 15
May 2018

application.

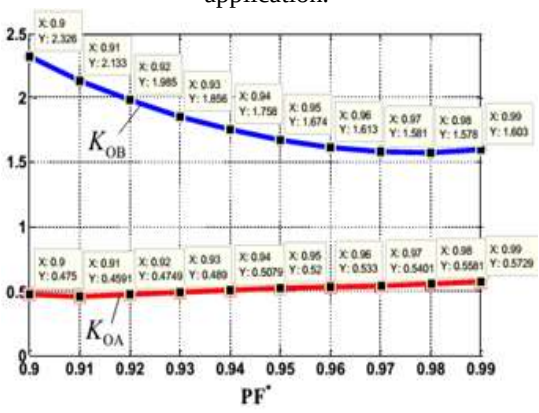

Fig. 6. The curves of slope-AO (i.e., KOA) and BO (i.e., KOB) v.s. PF

D. Negative Sequence Standard Consideration

From (16), the primary NSC I- can be calculated as:

$$I_{-}=\frac{1}{\sqrt{3}N}\sqrt{\xi_1^2+\xi_2^2}\,(I_{L\alpha p}+I_{L\beta p}), \qquad (19)$$

Where

$$\begin{cases}\xi_1=\mu_\alpha[\tan\delta_\beta\cos\Delta_\beta-\sin\Delta_\beta]+\mu_\beta[\cos(\Delta_a+30^\circ)+\tan\delta_a\sin(\Delta_a+30^\circ)]\\ \xi_2=\mu_\beta[\tan\delta_a\cos(\Delta_a+30^\circ)-\sin(\Delta_a+30^\circ)]-\mu_\alpha[\tan\delta_\beta\sin\Delta_\beta+\cos\Delta_\beta]\end{cases}$$

The negative sequence capacity S- in the primary side is

$$S_{-}=\sqrt{3}V_{sN}I_{-}=\sqrt{\xi_1^2+\xi_2^2}\,(P_{L\alpha}+P_{L\beta})=K(P_{L\alpha}+P_{L\beta}). \qquad (20)$$

Considering the Chinese national standard of the negative sequence component is

$$V_{unb}=\frac{V_{-}}{V_{+}}=\frac{S_{-}}{S_d}\le\varepsilon_V=2\%, \qquad (21)$$

Where V - and V+ are the primary negative and positive voltages, Sd is the short out limit of the footing substation.

The negative sequence prerequisite of the proposed system can be figured by joining (20) and (21), i.e.,

$$K(P_{L\alpha}+P_{L\beta})\le S_d\times 2\%. \qquad (22)$$

Fig. 7 gives the two phase loads' distribution graph of a genuine V/v transformer based footing substation (see Table II). The measurement results of Fig. 7 demonstrate that right around 95.2% of the load points are situated in the rectangle zone of CEDO, where the likelihood of the points distributed in ΔACO and ΔABO (or ΔAB1O, or ΔAB2O) is around 85%. Besides, we can likewise locate that, surpassing half of the load points are situated at stake OC and OD (take note of: a few points are covered on these two lines), which means the V/v transformer's ability usage ratio can be additionally improved in a vast potential. Based on the above measurement results, our consideration ought to be centered around the loads situated in CEDO and its limits.

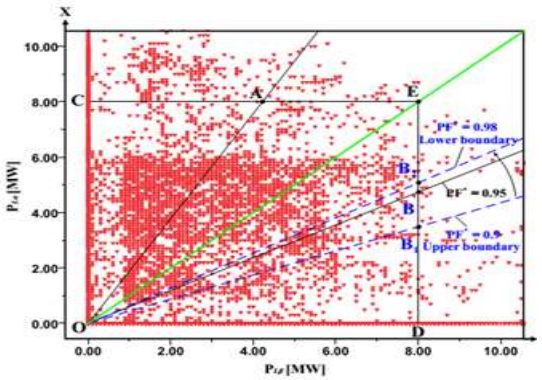

Fig. 7. The two phase load's distribution of a real V/v transformer based traction substation.

The surface of S - versus PLα and PLβ (inside rectangle region of CEDO appeared in Fig. 7) can be gotten based on (20) and the Sd given in Table II, which is appeared in Fig. 8. From the state of the surfaces appeared in Fig. 8, it can be reasoned that the maximum S - of Model-3, 2, and 4 happens on the point A, B, and E for any given PF*, individually.

Table II
The Specification Of A Real V/V Transformer

Grid line voltage	110kV
Transformer Capacity	20MVA phase-α: 10MVA phase-β: 10MVA
S_d of the traction substation	486MVA
Short circuit impendence	phase-α and β: 10%
Turn's ratio	110kV:27.5kV

The surface of S - vs. PLα and PLβ (within rectangle area of CEDO shown in Fig. 7) can be

International Journal of Research
Available at https://edupediapublications.org/journals
e-ISSN: 2348-6848
p-ISSN: 2348-795X
Volume 05 Issue 15
May 2018

obtained based on (20) and the Sd given in Table II, which is shown in Fig. 8. From the shape of the surfaces shown in Fig. 8, it can be concluded that the maximum S - of Model-3, 2, and 4 occurs on the point A, B, and E for any given PF*, respectively.

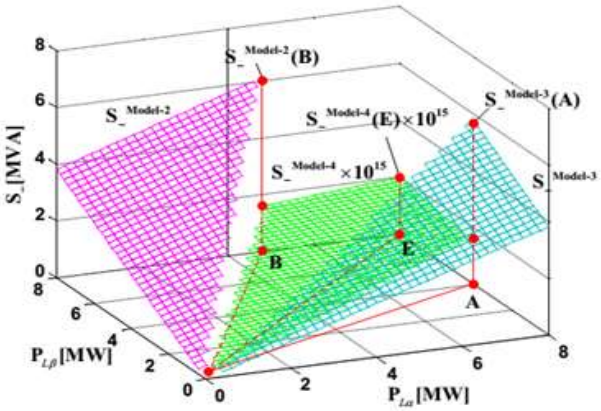

Fig. 8. The relationship of S- with PLα and PLβ (note: PF*=0.95)

Fig. 9 gives the relationship of the S-in A, B, and E, i.e., the maximum S - , S-max, with PF* for this footing substation in Model-2~4. Clearly, the S-blocking capacity of Model-4 is greatly improved than that of Model-3 and 2, however the last's S-max diminishes when PF* turns out to be extensive. Fig. 9 additionally demonstrates that the maximum negative sequence powers controlled by OSC are not as much as the authorization esteem 9.72MVA (i.e., 486MVA×2%), which means the Chinese national standard can be fulfilled when PF* is set inside 0.9 to 0.99. It ought to be commented here is that, if the authorization line of S-crosses with other maximum Sline of Model-2 or 3 appeared in Fig. 9, the correct hand abscissa of that intersection point ought to be chosen as the important PF*, on the grounds that the left one will lead Vunb out of the utmost.

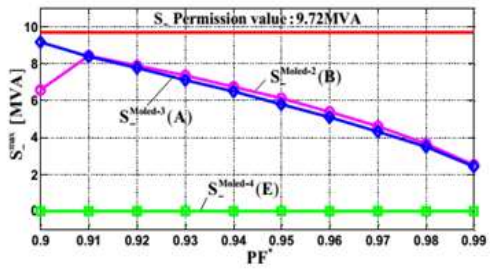

Fig. 9.The relationship of the primary maximum negative capacity with PF* in Modle-2, 3, and 4

The limit usage ability of RPFC ought to likewise be incorporated into our concerning degree. From Fig. 10, the maximum SRPFC's (i.e., SRPFCmax) lessening ratio diminishes intensely when PF*>0.95 [note: the maximum SRPFC point in PLα-PLβ panel (i.e., Fig. 7) is marked in Fig. 10]. In addition, RPFC's planning limit SRPFCdesign's diminishing ratio additionally indicates generally huge esteem (>23.43%) when PF*∈[0.9,0.95], it increments when PF*→0.9 [note: ①SRPFCdesign=2×maxthis is on the grounds that IGBT is a voltage touchy gadget and the dc-link voltages of converter-α and β are the same; ② Eα in Fig.10 means the maximum converter limit has a place with converter-α situated in point E]. Considering cost-productivity, PF* can be chosen from 0.9 to 0.95 for this footing substation.

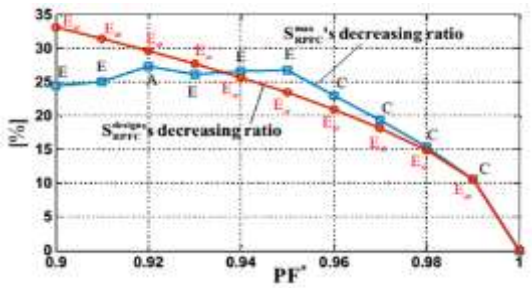

Fig. 10. The relationship of SRPFCmax's reducing ratio [1-maximum SRPFC/FCM based maximum SRPFC] and SRPFCdesign's reducing ratio [1-SRPFCdesign /FCM based SRPFCdesign] with PF* under the control of OCS.

E.Control Strategy Realization

The control system of the RPFC is plotted in Fig. 11. A few particulars ought to be made for it: The FFT strategy or the instantaneous reactive power theory [37] can be utilized for the estimation of the load's active and reactive power in the "PQ block", while the relative resounding controller (PS) is received as the present controller for its great following capacity in sing phase system. For the adjustment of vdc in the back-to - back system, rather than the figured Pcα, the genuine Pcα is produced by the dc-link voltage PI controller in converter-α. Furthermore, more consideration must be paid on the acknowledgment of the "repaying power figuring" block, and the accompanying four steps can help us to get the objective:

1) According the deliberate two phase loads (e.g., Fig. 7), Sd, and the exhibited slops of OA and OB appeared in Fig. 6, the PF*'s directing extent can be

resolved for the motivations behind fulfilling the negative sequence's standard (e.g., Fig. 9) and having generally little limit (e.g., Fig. 10).

2) Based on the pre-set PF* (e.g., PF*ϵ[0.9,0.95]), the inclines of OA and OB can be resolved from Fig. 6.
3) The remunerating model of OCS can be controlled by the load point's area in the load distribution panel appeared in Fig. 5 or 7, which can be reasoned by distinguishing the two phase loads' active power PLα, PLβ, and the slops of OA and OB pre-gotten in step 2.

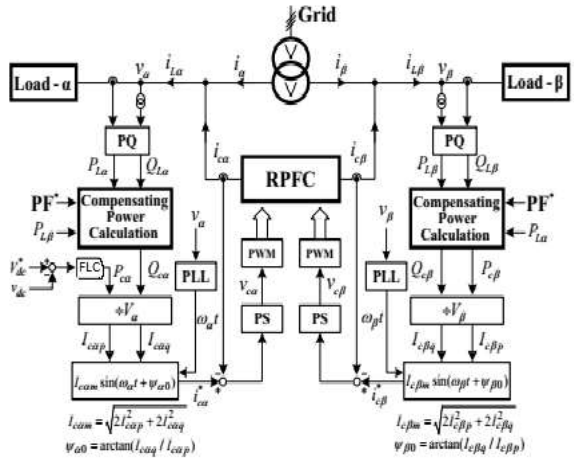

Fig. 11. The control system of the OCS based RPFC.

4) If the repaying model is gotten from step 3, φa, φb, and φc can be figured from Table I and (13), so as μα and μβ [see (10)]. Consequently, the repaying active and reactive power of RPFC can be at long last gotten from (12), [note: in (12), φLα=arctan(QLα/PLα), φLβ=arctan(QLβ/PLβ)].

IV. FUZZY LOGIC CONTROLLER

In FLC, basic control action is determined by a set of linguistic rules. These rules are determined by the system. Since the numerical variables are converted into linguistic variables, mathematical modeling of the system is not required in FC.

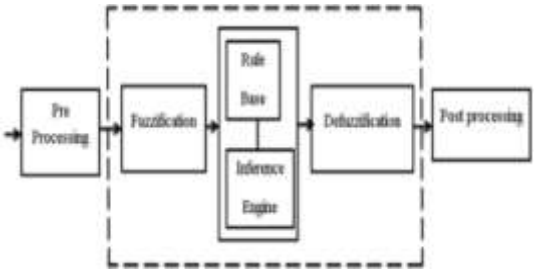

Fig.12.Fuzzy logic controller

The FLC comprises of three parts: fuzzification, interference engine and defuzzification. The FC is characterized as i. seven fuzzy sets for each input and output. ii. Triangular membership functions for simplicity. iii. Fuzzification using continuous universe of discourse. iv. Implication using Mamdani's, 'min' operator. v. Defuzzification using the height method.

TABLE III Fuzzy Rules

Change in error	Error						
	NB	NM	NS	Z	PS	PM	PB
NB	PB	PB	PB	PM	PM	PS	Z
NM	PB	PB	PM	PM	PS	Z	Z
NS	PB	PM	PS	PS	Z	NM	NB
Z	PB	PM	PS	Z	NS	NM	NB
PS	PM	PS	Z	NS	NM	NB	NB
PM	PS	Z	NS	NM	NM	NB	NB
PB	Z	NS	NM	NM	NB	NB	NB

Fuzzification: Membership function values are assigned to the linguistic variables, using seven fuzzy subsets: NB (Negative Big), NM (Negative Medium), NS (Negative Small), ZE (Zero), PS (Positive Small), PM (Positive Medium), and PB (Positive Big). The Partition of fuzzy subsets and the shape of membership *CE(k) E(k)* function adapt the shape up to appropriate system. The value of input error and change in error are normalized by an input scaling factor.

In this system the input scaling factor has been designed such that input values are between -1 and +1. The triangular shape of the membership function of this arrangement presumes that for any particular *E(k)* input there is only one dominant fuzzy subset. The input error for the FLC is given as

$$E(k) = \frac{P_{ph(k)} - P_{ph(k-1)}}{V_{ph(k)} - V_{ph(k-1)}} \quad (23)$$

$$CE(k) = E(k) - E(k\text{-}1) \quad (24)$$

Inference Method: Several composition methods such as Max–Min and Max-Dot have been proposed in the literature. In this paper Min method is used. The output membership function of each rule is given by the minimum operator and maximum operator. Table 1 shows rule base of the FLC.

International Journal of Research
Available at https://edupediapublications.org/journals
e-ISSN: 2348-6848
p-ISSN: 2348-795X
Volume 05 Issue 15
May 2018

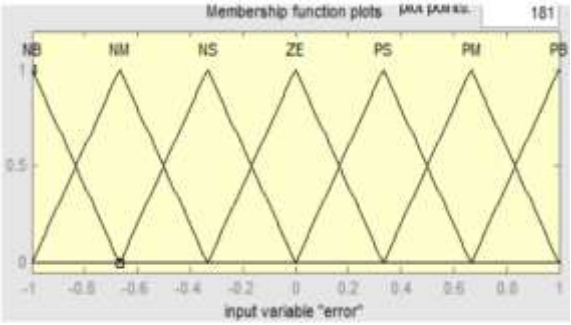

Fig.13.Membership functions

Defuzzification: As a plant usually requires a non-fuzzy value of control, a defuzzification stage is needed. To compute the output of the FLC, „height" method is used and the FLC output modifies the control output. Further, the output of FLC controls the switch in the inverter. In UPQC, the active power, reactive power, terminal voltage of the line and capacitor voltage are required to be maintained. In order to control these parameters, they are sensed and compared with the reference values. To achieve this, the membership functions of FC are: error, change in error and output

The set of FC rules are derived from

$$u=-[\alpha E + (1-\alpha)*C] \quad (24)$$

Where α is self-adjustable factor which can regulate the whole operation. E is the error of the system, C is the change in error and u is the control variable. A large value of error E indicates that given system is not in the balanced state. If the system is unbalanced, the controller should enlarge its control variables to balance the system as early as possible. One the other hand, small value of the error E indicates that the system is near to balanced state.

V. SIMULATION RESULTS

To approve the proposed OCS, the simulation model of the examined system appeared in Fig. 1 has been set up. The parameters of the main transformer, isolation transformer (IT), and converter are recorded in Tables II and III. Fig. 12, Table IV and Fig. 13, Table V are the simulation results in two cases. Fig. 12 compares the variable PF constant load, while the contrary condition has a place with Fig. 13. Figs. 12 and 13 demonstrate that, regardless of the two phase loads change or not, the primary PF move alongside PF* with the satisfactory execution [Fig. 12(b) and Fig. 13(b)]. Also, iA, iB, and iC have a tendency to be the adjusted three phase currents when PF* wound up bigger [Fig. 12(a) and Fig. 13(a)], which drives Vunb%≤2% [Fig. 12(c) and Fig. 13(c)]. Under the administration of OCS, we can likewise observe from Fig. 12(d) and Fig. 13(d) that SRPFC in a wide range of working conditions are not as much as that in FCM, e.g., Fig. 12(d), 0.4-0.6s: SRPFC|PF*=0.95= 0.72SRPFC|PF*=1,Fig. 13(d), 1-1.2s: SRPFC|PF*=0.95=0.73SRPFC|PF*=1; it is incidental with the hypothetical investigation stated in Section III.

Table IV
The Parameters Of The Isolation Transformer And Rpfc

The VA-capacity of IT	5MVA
Short circuit impendence of IT	21%
IT's turn's ratio [a]	27.5kV:27.5kV
The dc-link voltage of RPFC	51.15kV

Table V
Action Sequence Of The Case Shown In Fig. 12

Time	PF*	Compensation model	Load condition
0.0-0.2s	No RPFC	-	P_{La}=8MW, Q_{La}=6Mvar; $P_{Lβ}$=0MW, $Q_{Lβ}$=0Mvar
0.2-0.4s	0.90	Model-3	
0.4-0.6s	0.95	Model-3	
0.6-0.8s	0.97	Model-3	
0.8-1.0s	1.00	FCM	

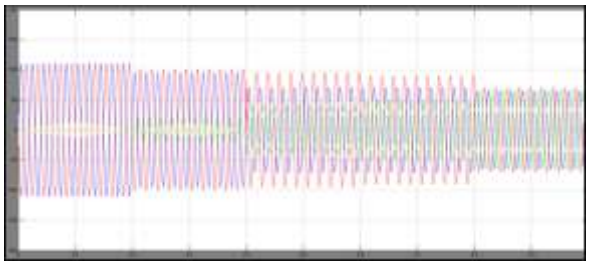
(a)

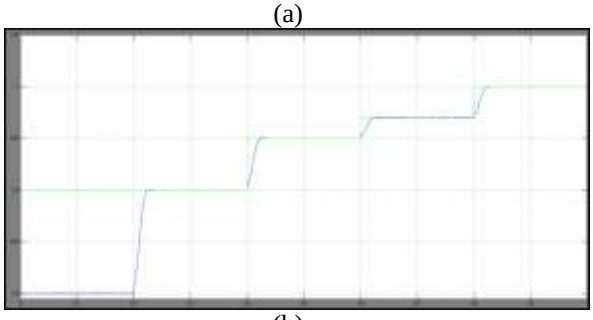
(b)

International Journal of Research
Available at https://edupediapublications.org/journals
e-ISSN: 2348-6848
p-ISSN: 2348-795X
Volume 05 Issue 15
May 2018

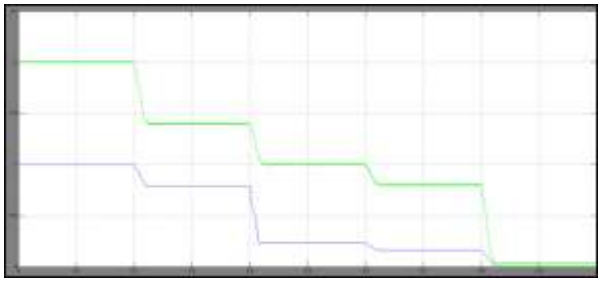

(c)

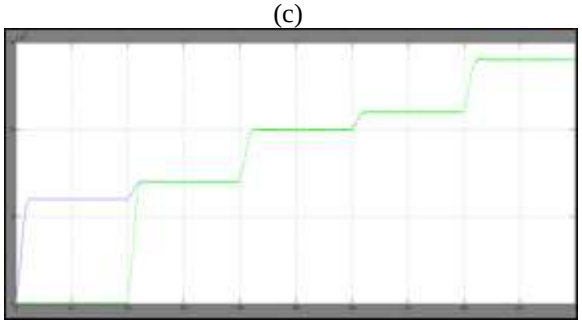

Fig. 12.The waveforms in the con
dition of variable PF* with constant load. (a) Primary three phase currents. (b) PF* and PF. (c) Voltage's and current's unbalanced ratio. (d) Capacity of RPF

Table VI
Action Sequence Of The Case Shown In Fig. 13

Time	Load condition	PF*	Compensation model
0.0-0.2s	P_{La}=0MW, Q_{La}=0Mvar; $P_{Lß}$=8MW, $Q_{Lß}$=6Mvar	No RPFC	-
0.2-0.4s	P_{La}=0MW, Q_{La}=0Mvar; $P_{Lß}$=8MW, $Q_{Lß}$=6Mvar	1	FCM
0.4-0.6s	P_{La}=8MW, Q_{La}=6Mvar; $P_{Lß}$=8MW, $Q_{Lß}$=6Mvar		
0.6-0.8s	P_{La}=8MW, Q_{La}=6Mvar; $P_{Lß}$=0MW, $Q_{Lß}$=0Mvar		
0.8-1.0s	P_{La}=0MW, Q_{La}=0Mvar; $P_{Lß}$=8MW, $Q_{Lß}$=6Mvar	0.95	Model-2
1.0-1.2s	P_{La}=8MW, Q_{La}=6Mvar; $P_{Lß}$=8MW, $Q_{Lß}$=6Mvar		Model-4
1.2-1.4s	P_{La}=8MW, Q_{La}=6Mvar; $P_{Lß}$=0MW, $Q_{Lß}$=0Mvar		Model-3

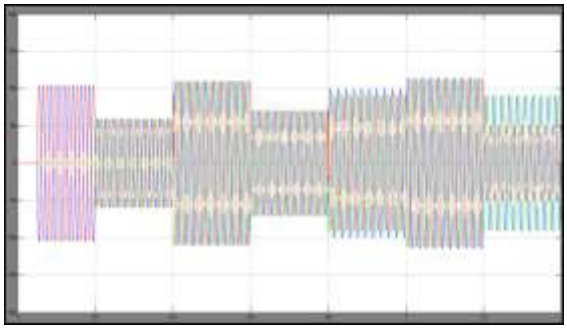

(a)

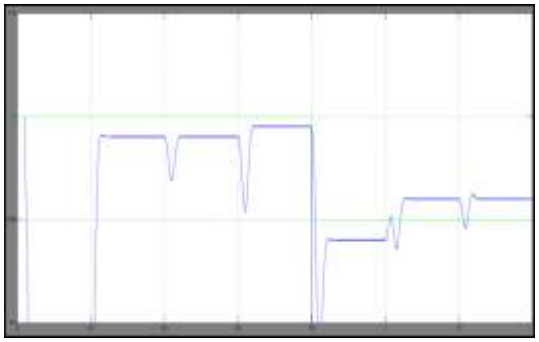

(b)

(c)

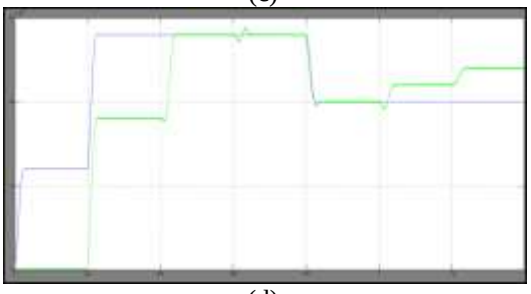

(d)

Fig. 13.The waveforms in the condition of variable load with constant PF*. (a) Primary three phase currents. (b) PF* and PF. (c) Voltage's and current's unbalanced ratio. (d) Capacity of RPFC.

VI. CONCLUSION

This paper proposed a power factor arranged RPFC for the power quality improvement in the normal utilized two phase cargo prepare ruled ERPS. The mathematical model of the RPFC coordinated ERPS and the far reaching plan technique for the proposed control methodology are given in detail, based on a genuine footing substation. The simulation and the exploratory results confirm the accuracy of the proposed considers. In the start of fulfilling the norms of the reactive power and NSV, this paper gives an ideal control technique for the PQ improvement, control adaptability upgrade, and the lessening of RPFC's remunerating and planning limit in two or single phase RPFC incorporated ERPS. In

other words, this control technique can influence the system to have an attractive high cost-effectiveness in two or single phase footing load conditions.

REFERENCES

[1] S. Chen, R. Li, and H.4 Hsiang, "Traction system unbalance problemanalysis methodologies," IEEE Trans. Power Del., vol. 19, no. 4, pp. 1877–1883, Oct. 2004.

[2] J. Kilter, T. Sarnet, and T. Kangro, "Modelling of high-speed electrical railway system for transmission network voltage quality analysis: Rail Baltic case study," in Proc. Elect. Power Qual. Supply Reliab. Conf. (PQ), 2014, pp. 323–328.

[3] Z. He, H. Hu, Y. Zhang, and S. Gao, "Harmonic resonance assessment to traction power-supply system considering train model in China high-speed railway," IEEE Trans. Power Del., vol. 29, no. 4, pp. 1735– 1743, Aug. 2014.

[4] G. Raimondo, P. Ladoux, A. Lowinsky, H. Caron, and P. Marino, "Reactive power compensation in railways based on AC boost choppers," IET Electr. Syst. Transp., vol. 2, no. 4, pp. 169–177, Jua. 2012.

[5] Z. Zhang, Y. Li, L. Luo, P. Luo, Y. Cao, Y. Chen et al, "A new railway power flow control system coupled with asymmetric double LC branches," IEEE Trans. Power Electron., vol. 30, no. 10, pp. 5484–5498, Oct. 2015.

[6] S. Gazafrudi, A. Langerudy, E. Fuchs, and K. Al-Haddad, "Power quality issues in railway electrification: a comprehensive perspective," IEEE IEEE Trans. Ind. Electron., vol. 62, no. 5, pp. 3081–3090, May. 2015.

[7] T. Uzuka, "Faster than a speeding Bullet: An overview of Japanese high-speed rail technology and electrification," IEEE Electrification Mag., vol.1, no.1, pp. 11–20, Sep. 2013.

[8] M. Brenna, F. Foiadelli, and D. Zaninelli, "Electromagnetic model of high speed railway lines for power quality studies," IEEE Trans. Power Syst., vol. 25, no. 3, pp. 1301–1308, Aug. 2010.

[9] H. Wang, Y. Liu, K. Yan, Y. Fu, and C. Zhang, "Analysis of static VAr compensators installed in different positions in electric railways," IET Elect. Syst. Transp., vol. 5, no. 3, pp. 129–134, Jan. 2015.

[10] G. Zhu, J. Chen, and X. Liu, "Compensation for the negative-sequence currents of electric railway based on SVC," in Proc. ICIEA. Conf., 2008, pp. 1958–1963.

[11] K. Fujii, K. Kunomura, K. Yoshida, A. Suzuki, S. Konishi, M. Daiguji et al., "STATCOM applying flat-packaged IGBTs connected in series," IEEE Trans. Power Electron., vol. 20, no. 5, pp. 1125–1132, Sep. 2005.

[12] R. Grunbaum, J. Hasler, T. Larsson, and M. Meslay, "STATCOM to enhance power quality and security of rail traction supply," in Proc. 8th Int. Symp.Adv. Electro-Mech. Motion Syst. Electr.Drives, Lille, France, 2009, pp. 1–6.

[13] A. Bueno, J. Aller; J. Restrepo, R. Harley, T. Habetler, "Harmonic and unbalance compensation based on direct power control for electric railway systems," IEEE Trans. Power Electron., vol.28, no.12, pp. 5823-5831, Dec. 2013.

[14] B. Gultekin, C. Gercek, T. Atalik, M. Deniz, N. Bicer, M. Ermis et al., "Design and implementation of a 154-kV ±50-Mvar transmission STATCOM based on 21-level cascaded multilevel converter," IEEE Trans. Ind. Appl., vol. 48, no. 3, pp. 1030–1045, May. 2012.

[15] P. Ladoux, G. Raimondo, H. Caron, and P. Marino, "Chopper-controlled steinmetz circuit for voltage balancing in railway substations," IEEE Trans. Power Electron., vol. 28, no. 12, pp. 5813–5882, Dec. 2013.

GADAPA NARESH has completed B.Tech in Electrical & Electronics Engineering in 2015 from Malla Reddy institute of Education and Technology affiliated to JNTUH, Hyderabad and Pursuing M.Tech from VidyaJyothi Institute of Technology (Autonomous), Hyderabad, Telangana, India. Area of interest includes Power Electronics, Electrical Drives, Machines.
E-mail id:nareshgadapa715@gmail.com.

P.NAGESWARA RAO is an Associate Professor working with VidyaJyothi Institute of Technology ,Hyderabad India in the Electrical and Electronics Engineering Department . His areas of interests are power systems & power electronics.